EPJ manuscript No.
(will be inserted by the editor)

T-matrix approach to heavy quark diffusion in the QGP

H. van Hees[1], M. Mannarelli[2], V. Greco[3], and R. Rapp[4]

[1] Institut für Theoretische Physik, Justus-Liebig-Universität Giessen, Heinrich-Buff-Ring 16, D-35392 Giessen, Germany
[2] Instituto de Ciencias del Espacio (IEEC/CSIC), E-08193 Bellaterra (Barcelona), Spain
[3] Dipartimento di Fisica e Astronomia, Via S. Sofia 64, I-95125 Catania, Italy
[4] Cyclotron Institute and Physics Department, Texas A&M University, College Station, Texas 77843-3366, U.S.A.

August 27, 2008

Abstract. We assess transport properties of heavy quarks in the Quark-Gluon Plasma (QGP) using static heavy-quark (HQ) potentials from lattice-QCD calculations in a Brueckner many-body T-matrix approach to evaluate elastic heavy-quark-light-quark scattering amplitudes. In the attractive meson and diquark channels resonance states are formed for temperatures up to $\sim 1.5T_c$, increasing pertinent drag and diffusion coefficients for heavy-quark rescattering in the QGP beyond the expectations from perturbative-QCD calculations. We use these transport coefficients, complemented with perturbative elastic HQ gluon scattering, in a relativistic Langevin simulation to obtain HQ p_t distributions and elliptic flow (v_2) under conditions relevant for the hot and dense medium created in ultrarelativistic heavy-ion collisions. The heavy quarks are hadronized to open-charm and -bottom mesons within a combined quark-coalescence fragmentation scheme. The resulting single-electron spectra from their semileptonic decays are confronted with recent data on "non-photonic electrons" in 200 AGeV Au-Au collisions at the Relativistic Heavy-Ion Collider (RHIC).

1 Introduction

One of the most interesting questions in high-energy nuclear physics is that about the properties of the hot and dense medium created in ultra-relativistic heavy-ion collisions. Finite-temperature lattice-QCD (lQCD) calculations of strongly-interacting matter predict a phase transition from hadronic matter to a quark-gluon plasma (QGP) at a critical temperature, $T_c \simeq 180$ MeV [1]. In the recent years the experimental program at the Relativistic Heavy-Ion collider has resulted in convincing evidence for the formation of such a hot and dense partonic state [2,3,4,5].

The heavy charm and bottom quarks are particularly valuable probes for the properties of this medium since they are created in the primordial hard collisions of the nucleons within the colliding nuclei. Thus, they form a rather well defined initial state and interact with the hot and dense fireball during its entire evolution. Recently, measurements of the transverse-momentum distributions of "non-photonic single electrons" ($e^{\pm}$), which originate mainly from the semi-leptonic decays of open-charm and -bottom mesons, in 200 AGeV Au-Au collisions at RHIC have found a surprisingly large suppression at high transverse momenta (p_t) (i.e., a small nuclear modification factor, R_{AA}) and a large elliptic-flow parameter, v_2. Both findings indicate that during the lifetime of the hot and dense fireball heavy quarks come close to thermal equilibrium with the medium [6,7,8].

The theoretical challenge is to understand the corresponding thermalization times of heavy quarks from the underlying microscopic scattering processes with the constituents of the QGP, in particular how the heavy quarks, despite their large masses, $m_Q \gg T_c$, become part of the collective flow of the fireball. In calculations of the pertinent transport coefficients from perturbative QCD (pQCD), based on gluon-bremsstrahlung energy loss, including elastic HQ scattering, one has to artificially tune the coupling strength beyond the applicability range of perturbation theory [9,10]. It has also been shown that the convergence of the perturbative series for the HQ diffusion coefficient is quite poor [11]. Thus, non-perturbative approaches have to be used to explain the strong HQ couplings necessary. One suggested mechanism is the formation of D- and B-meson resonance excitations in the deconfined phase of QCD matter [12,13] which has lead to a quite satisfactory description of the $e^{\pm}$ data at RHIC.

This paper is organized as follows: In Sec. 2 we use HQ static potentials from lattice-QCD calculations at finite temperature in a many-body Brueckner T-matrix approach to calculate elastic HQ light-quark scattering-matrix elements in the medium [14,15]. We show that after inclusion of a complete set of color channels, taking into account $l = 0, 1$ states in the partial-wave expansion of the T-matrix, the resonance states, conjectured in the earlier approaches, are confirmed by these interactions, which are in principle free of tunable parameters. The resulting elastic-scattering amplitudes are used in Sec. 3 to calculate

drag and diffusion coefficients for a Fokker-Planck equation [16,12,17], describing the rescattering of the heavy quarks within the hot and dense sQGP fireball. In the next step we employ a relativistic Langevin simulation to find the corresponding HQ p_t distributions, using a thermal-fireball parameterization, including elliptic flow for non-central heavy-ion collisions. To confront these spectra with the $e^{\pm}$ data from the PHENIX and STAR collaborations at RHIC, in Sec. 4 we use a combined quark-coalescence and fragmentation model to hadronize the heavy quarks to D and B mesons which then are decayed semi-leptonically leading to the final $e^{\pm}$ spectra which can be directly confronted with recent data on nonphotonic single electrons in 200 AGeV Au-Au collisions at RHIC. The paper closes with brief conclusions and an outlook (Sec. 5).

2 HQ scattering in the QGP

In this Sec. we calculate in-medium matrix elements for elastic scattering of heavy quarks ($Q = c, b$) with light quarks $q = u, d, s$ in a Brueckner-like many-body approach, assuming that a static heavy-quark light-quark potential, $V(r)$, can be employed as the interaction kernel. Such a model has been used in the vacuum to successfully describe D-meson spectra and decays [18,19]. Further, we assume that the effective in-medium potential can be extracted from finite-temperature lQCD calculations of the color-singlet free energy $F_1(r,T)$ [20,21] for a static $\bar{Q}Q$ pair as the internal potential energy by the usual thermodynamic relation [14,22,23,24],

$$U_1(r,T) = F_1(r,T) - T\frac{\partial F_1(r,T)}{\partial T}. \tag{1}$$

For application as a scattering kernel in a T-matrix equation, the potential as to vanish for $r \to \infty$. Thus we choose the accordingly subtracted internal potential energy,

$$V_1(r,T) = U_1(r,T) - U_1(r\to\infty,T). \tag{2}$$

In lQCD simulations one finds that $U_1(r \to \infty, T)$ is a decreasing function with temperature which could be associated as a contribution to the in-medium HQ mass, $m_Q(T) = m_0 + U_1(r \to \infty, T)/2$ where m_0 denotes the bare mass. However, this leads to problems since close to T_c the asymptotic value, $U_1(r \to \infty, T)$, develops a pronounced peak structure. Thus, in this calculation, we assume constant effective HQ masses, $m_c = 1.5$ GeV and $m_b = 4.5$ GeV.

We also consider the complete set of color channels for the $Q\bar{q}$ (singlet and octet) and Qq (anti-triplet and sextet) systems, using Casimir scaling as in leading-order pQCD,

$$V_8 = -\frac{1}{8}V_1, \quad V_{\bar{3}} = \frac{1}{2}V_1, \quad V_6 = -\frac{1}{4}V_1, \tag{3}$$

which is also justified by recent lQCD calculations of the finite-T HQ free energy [25,26].

This approach is in principle parameter free in the choice of the interactions, since their strength is taken from first-principle lQCD simulations. However, there are considerable uncertainties in the potentials (a) between different lattice calculations and (b) in the extraction and parameterization of the corresponding free energies, particularly their temperature dependence needed to subtract the entropy term in Eq. (1). In addition, the very notion of an "in-medium potential" is not a unique concept [27], and its identification with the internal potential energy may be seen as an upper limit in interaction strength. We use three different parameterizations of F_1 [23,22,14]:

[Wo] of quenched lQCD [20],
[SZ] of two-flavor lQCD [28], and
[MR] of three-flavor lQCD [29].

The resulting potentials from [Wo] and [SZ] are comparable to a numerical extraction from three-flavor lQCD [29], while that from [MR] is deeper than the other two for $T \lesssim 1.6T_c$, but falls off faster at higher temperatures. The resulting uncertainty in the transport coefficients (see Sec. 3) amounts to up to 40%. To define the Brueckner-type many-body scheme the four-dimensional (4D) Bethe-Salpeter (BS) ladder approximation, symbolized in diagrammatical form by the upper panel of Fig. 1, has to be reduced to a 3D Lippmann-Schwinger (LS) equation, neglecting antiparticle components in the quark propagators, in order to implement the static potential from lQCD via Eqs. (1-3). After this reduction the LS equation in the color channel, $a \in \{1, \bar{3}, 6, 8\}$ reads [14][1]

$$\begin{aligned} T_a(E;\boldsymbol{q}',\boldsymbol{q}) =& V_a(\boldsymbol{q}',\boldsymbol{q}) - \int \frac{\mathrm{d}^3\boldsymbol{k}}{(2\pi)^3} V_q(\boldsymbol{q}',\boldsymbol{k}) G_{qQ}(E;k) \\ & \times T_a(E;\boldsymbol{k},\boldsymbol{q})[1 - f_F(\omega_k^q) - f_F(\omega_k^Q)] \end{aligned} \tag{4}$$

with the Fourier-transformed potentials,

$$V_a(\boldsymbol{q}',\boldsymbol{q}) = \int \mathrm{d}^3\boldsymbol{r} V_a(r) \exp[\mathrm{i}(\boldsymbol{q}-\boldsymbol{q}')\boldsymbol{r}]. \tag{5}$$

Further, E, $\boldsymbol{q}$ and $\boldsymbol{q}'$ denote the energy and incoming and outgoing momenta in the center-of-mass (CM) frame, re-

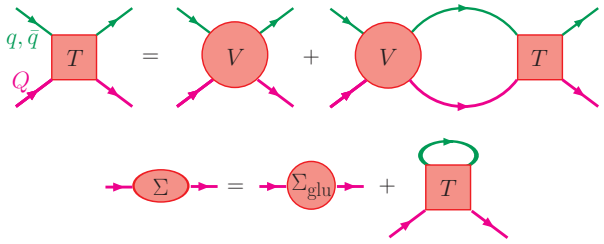

Fig. 1. (Color online) Diagrammatic representation of the Brueckner many-body scheme for the coupled system of the T-matrix based on the lQCD static internal potential energy as the interaction kernel and the HQ self-energy.

[1] Here and in the following all vertex and Green's functions are understood as the retarded real-time quantities which can be derived as analytic continuations of the corresponding imaginary-time (Matsubara) quantities of thermal quantum field theory.

spectively.

$$f_F = \frac{1}{\exp(\omega/T)+1} \tag{6}$$

is the Fermi-Dirac distribution. The quark-dispersion relations are determined in quasi-particle approximation by

$$\omega_k^{q,Q} = \sqrt{k^2 + m_{q,Q}^2}, \tag{7}$$

where for simplification we do not solve the fully self-consistent scheme in Fig. 1 but use a fixed mass of $m_q = 0.25$ GeV, $m_c = 1.5$ GeV, and $m_b = 4.5$ GeV for the light, charm, and bottom quarks, respectively. Finally, the two-particle-qQ propagator in (4) is given in terms of the Thompson-reduction scheme [30]

$$G_{qQ}(E;k) = \frac{1}{4}\frac{1}{E-(\omega_k^q + \mathrm{i}\Sigma_I^q) - (\omega_k^Q + \mathrm{i}\Sigma_I^Q)} \tag{8}$$

with a quasi-particle width for both light and heavy quarks of $-2\Sigma_I^{q,Q} = 0.2$ GeV.

The solution of the LS equation (4) is simplified by using a partial-wave expansion of the potential and T-matrix,

$$\begin{aligned} V_a(\boldsymbol{q}',\boldsymbol{q}) &= 4\pi\sum_l (2l+1) V_{a,l}(q',q) P_l[\cos\angle(\boldsymbol{q},\boldsymbol{q}')], \\ T_a(E;\boldsymbol{q}',\boldsymbol{q}) &= 4\pi\sum_l (2l+1) T_{a,l}(E;q',q) P_l[\cos\angle(\boldsymbol{q},\boldsymbol{q}')], \end{aligned} \tag{9}$$

which leads to the 1D LS equations,

$$\begin{aligned} T_{a,l}(E;q',q) = V_{a,l}(q',q) + \frac{2}{\pi}\int \mathrm{d}k k^2 V_{a,l}(q',k) G_{Qq}(E;k) \\ \times T_{a,l}(E;k,q)[1 - f_F(\omega_k^Q) - f_F(\omega_k^q)], \end{aligned} \tag{10}$$

for the partial-wave components, $T_{a,l}$, of the T-matrix, which are solved numerically with the matrix-inversion algorithm of Haftel and Tabakin [31]. We restrict ourselves to S ($l=0$) and P ($l=1$) waves. As can be seen from Fig. 2, in the dominating attractive color-singlet $Q\bar{q}$ and color-antitriplet Qq channels, close to the critical temperature, $T_c \simeq 180$ MeV, resonance states above the threshold, $E_{\mathrm{thr}} = m_Q + m_q$ are formed, similar as conjectured in [12, 13]. However, in this full in-medium scheme the resonances melt at higher temperatures $T \gtrsim 1.7T_c$ and $T \gtrsim 1.4T_c$, respectively. As we shall see in the next section, contrary to the expectation from perturbative calculations, using the [Wo] parameterization of the potential, this leads even to *decreasing* transport coefficients with increasing temperature, i.e., the decreasing interaction strength of the potential overcompensates the higher density of the medium.

The HQ self-energy, diagrammatically represented by the lower panel of Fig. 1, is then given by

$$\begin{aligned} \Sigma_a^Q(\omega,p) = &\frac{d_{\mathrm{SI}} d_a}{6}\int \frac{k^2 \mathrm{d}k\mathrm{d}x}{4\pi^2}[f_F(\omega_k) + f_B(\omega+\omega_k)] \\ &\times T_a(E;\boldsymbol{p},\boldsymbol{k}), \end{aligned} \tag{11}$$

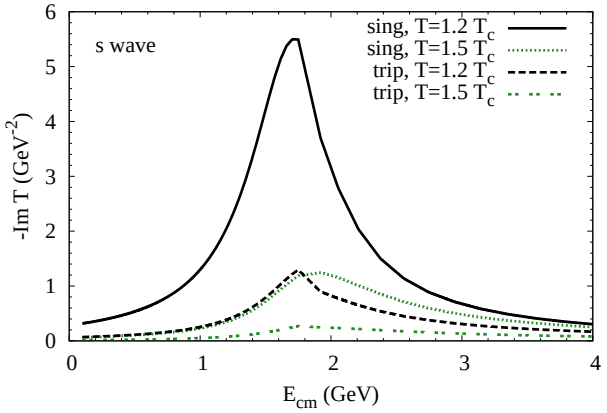

Fig. 2. (Color online) Imaginary part of the S-wave in-medium T matrix for $c\bar{q}$ and cq scattering in the color-singlet and -antitriplet channels based on the parameterization of the lQCD potential energy by [Wo].

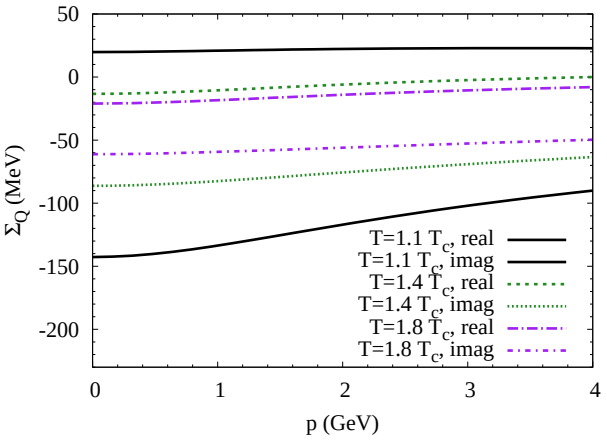

Fig. 3. (Color online) Real and imaginary parts of the c-quark self-energy as a function of three-momentum at different temperatures.

where $d_{\mathrm{SI}} = 4(2l+1)N_f$ denotes the spin-isospin degeneracy of the light quarks (which is already implicitly assumed in the light-heavy quark interaction of our approach, which is in line with the free D-meson spectrum [32]) in the l^{th} partial wave and d_a the color degeneracy in the corresponding channel. Here we assume an effective number of light-quark flavors, $N_f = 2.5$, to account for the smaller strange-quark density. For the charm quarks, cf. Fig. 3 the calculation leads to an in-medium width of $\Gamma_c = -2\,\mathrm{Im}\,\Sigma_c \simeq 200$ MeV, which justifies our simplifying assumption in the T-matrix calculation above.

3 HQ transport in the QGP

To evaluate the motion of the heavy quarks in the hot and dense fireball, consisting of light quarks and gluons, we employ a Langevin simulation of the Fokker-Planck equation,

$$\frac{\partial f_Q}{\partial t} = \frac{\partial}{\partial p_i}(p_i \gamma f_Q) + \frac{\partial^2}{p_i p_j}(B_{ij} f_Q). \tag{12}$$

The drag or friction coefficient, γ, and diffusion coefficients,

$$B_{ij} = B_0 \frac{p_i p_j}{p^2} + B_1 \left(1 - \frac{p_i p_j}{p^2}\right), \tag{13}$$

are calculated from the invariant scattering-matrix elements [16]. Taking into account elastic scattering of the heavy quark with a light quark or antiquark the latter given in terms of the above calculated T-matrix by

$$\sum |\mathcal{M}|^2 = \frac{64\pi}{s^2}(s - m_q^2 + m_Q^2)^2 (s - m_Q^2 + m_q^2)^2 \times N_f \sum_a d_a (|T_{a,l=0}(s)|^2 + 3|T_{a,l=1}(s)\cos(\theta_{\rm cm})|^2). \tag{14}$$

We define the averaging operator

$$\langle X(\boldsymbol{p})\rangle = \frac{1}{2E_p}\int \frac{\mathrm{d}^3\boldsymbol{q}}{(2\pi)^3 2E_q}\int \frac{\mathrm{d}^3\boldsymbol{q}'}{(2\pi)^3 2E_{q'}} \int \frac{\mathrm{d}^3\boldsymbol{p}'}{(2\pi)^3 2E_{p'}}\frac{1}{\gamma_c}\sum |\mathcal{M}|^2 (2\pi)^4\delta^{(4)}(p+q-p'-q')f_q(\boldsymbol{q})X(\boldsymbol{p}') \ , \tag{15}$$

for a heavy-quark observable, X, over the elastic scatterings per unit time of the heavy quark with momentum $\boldsymbol{p}$ with a light quark of momentum $\boldsymbol{q}$, changing their momenta to $\boldsymbol{p}'$ and $\boldsymbol{q}'$. Here, f_q is the (thermal) distribution of the light quarks in the medium. Then we can calculate the transport coefficients as

$$\gamma(|\boldsymbol{p}|) = \langle 1\rangle - \frac{\langle \boldsymbol{p}\cdot\boldsymbol{p}'\rangle}{\boldsymbol{p}^2}, \tag{16}$$

$$B_0(|\boldsymbol{p}|) = \frac{1}{4}\left[\langle \boldsymbol{p}'^2\rangle - \frac{\langle(\boldsymbol{p}\cdot\boldsymbol{p}')^2\rangle}{\boldsymbol{p}^2}\right], \tag{17}$$

$$B_1(|\boldsymbol{p}|) = \frac{1}{2}\left[\frac{\langle(\boldsymbol{p}\cdot\boldsymbol{p}')^2\rangle}{\boldsymbol{p}^2} - 2\langle \boldsymbol{p}'\cdot\boldsymbol{p}\rangle + \boldsymbol{p}^2\langle 1\rangle\right]. \tag{18}$$

However, it turns out that, in order to guarantee the proper equilibrium limit of the heavy quarks with the medium, we have to enforce Einstein's fluctuation-dissipation relation for the longitudinal diffusion coefficient, which is used here in its relativistic form [17,13],

$$B_1 = ET\gamma. \tag{19}$$

The nonperturbative HQ light-quark scattering-matrix elements are supplemented by the corresponding perturbative elastic HQ gluon-scattering ones [33]. The t-channel singularity is regulated by a gluon-Debye screening mass of $m_g = gT$ with a strong coupling constant $g = \sqrt{4\pi\alpha_s}$, using $\alpha_s = 0.4$. As shown in Fig. 4, close to T_c the equilibration times of $\tau_{\rm eq} = 1/\gamma \simeq 7$ fm/c for charm quarks are a factor of ~ 4 larger than the values from a corresponding pQCD calculation, reminiscent to the results based on the model, assuming the survival of D-meson like resonance states above T_c [12,13]. In contrast to this and other calculations of the HQ transport coefficients, here the drag coefficients *decrease* with increasing temperature because

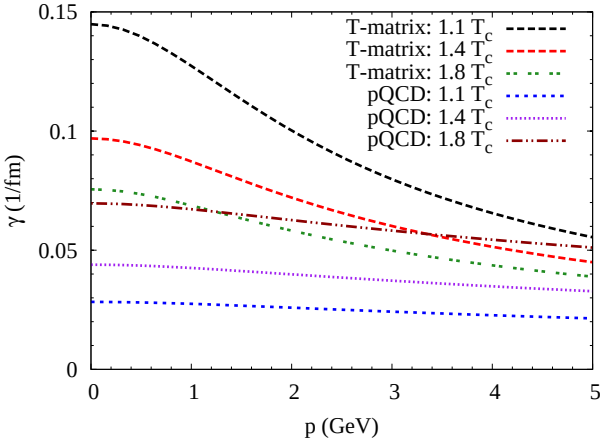

Fig. 4. (Color online) The drag coefficient, γ, as a function of HQ momentum, calculated via (16) with scattering-matrix elements from the non-perturbative T-matrix calculation (using the parameterization of the lQCD internal potential energies by [Wo]) compared to a LO perturbative calculation based on matrix elements from [33].

of the "melting" of the dynamically generated resonances at increasing temperatures due to the diminishing interaction strength from the lQCD potentials.

To solve the Fokker-Planck equation (12) under conditions of the sQGP medium produced in heavy-ion collisions, we use an isentropically expanding thermal fireball model, assuming an ideal-gas equation of state of $N_f = 2.5$ effective massless light-quark flavors and gluons. The total entropy is fixed by particle multiplicities at chemical freeze-out which we assume to occur at the critical temperature, $T_c = 180$ MeV. For semi-central collisions the fireball is chosen to be of elliptic-cylindrical shape with isobars given by confocal ellipses with a perpendicular radial-flow field, scaling linearly with the distance from the center as seen in hydrodynamic calculations [34] to which also the (average) radial flow velocity and ellipticity, v_2, is fixed. To compare to "minimum-bias" data on $e^{\pm}$ spectra in 200 AGeV Au-Au reactions at RHIC we simulate collisions with an impact parameter of $b = 7$ fm, implying an initial spatial eccentricity of about 0.6. Using a QGP-formation time of 0.33 fm/c leads to an initial temperature of 340 MeV. The evolution stops after the fireball has undergone a mixed QGP-hadronic phase after about 5 fm/c, at which the radial velocity of the fireball has reached about a radial velocity of about $v_\perp = 0.5c$ at the surface and an ellipticity of $v_2 = 5.5\%$.

Given this description of the medium, (12) is solved with help of an equivalent relativistic Langevin simulation which is defined by the stochastic equation of motion for a heavy quark at position, $\boldsymbol{x}$, and momentum $\boldsymbol{p}$:

$$\delta\boldsymbol{x} = \frac{p}{E}\delta t, \quad \delta\boldsymbol{p} = -\gamma(t,\boldsymbol{p})\boldsymbol{p}\delta t + \delta\boldsymbol{W}(t,\boldsymbol{p}+\delta\boldsymbol{p}), \tag{20}$$

where $\delta\boldsymbol{W}$ is a stochastic force distributed normally,

$$P(\delta\boldsymbol{W}) \propto \exp\left[-\frac{(B^{-1})_{jk}\delta W^j \delta W^k}{4\delta t}\right], \tag{21}$$

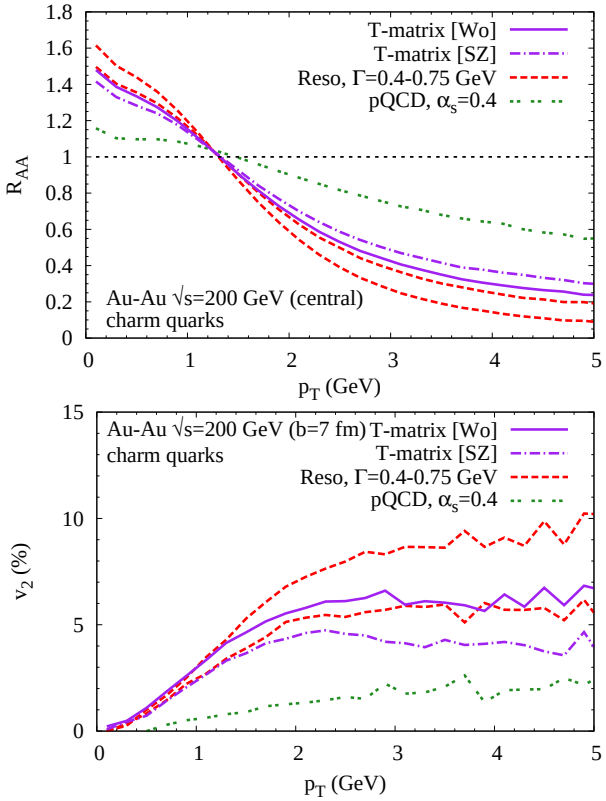

Fig. 5. (Color Online) Nuclear modification factor, R_{AA}, for central (upper panel) and elliptic flow, v_2, for semicentral (lower panel) 200 AGeV Au-Au collisions for charm quarks from the Langevin simulation, using the T-matrix results for the transport coefficients employing the parameterizations [Wo] and [SZ] for the lQCD potentials, compared to a calculation based on pQCD and the resonance-model interactions in [13]

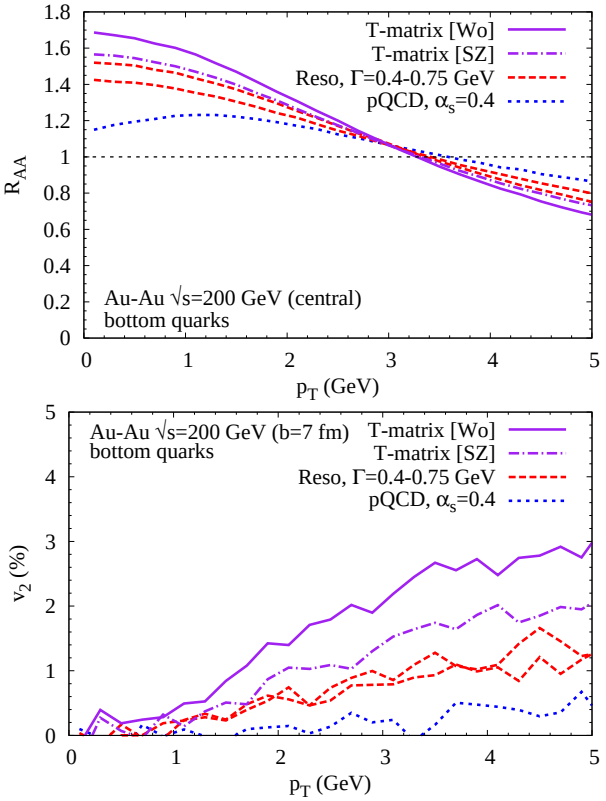

Fig. 6. (Color online) The same as Fig. 5 but for bottom quarks

B^{-1} denoting the inverse of the diffusion-coefficient matrix (13). Note that in (20) and (21) the diffusion coefficients are to be evaluated at the updated momenta $\boldsymbol{p}+\delta\boldsymbol{p}$. This Hänggi-Klimontovich realization of the stochastic process together with the dissipation-fluctuation relation (19) ensures the correct equilibrium limit in the long-time regime $t \gg 1/\gamma$ [35]. After evaluation of the time step (20) the resulting momenta are Lorentz boosted to the laboratory frame.

The initial condition for (20) is given by the phase-space distribution of the heavy quarks. The spatial distribution is determined with a Glauber model for heavy-quark production. The initial p_t spectrum is determined from data on p-p and d-Au collisions at RHIC as follows: The c-quark spectra are taken from a modified PYTHIA calculation to fit D and D^* spectra in d-Au collisions [36], assuming δ-function fragmentation. After decaying this spectrum to single $e^{\pm}$ they saturate corresponding data from p-p- and d-Au [6,37] collisions up to $p_t \simeq 3.5$ GeV. The missing yield at higher p_t is assumed to be filled with the corresponding contributions from B mesons, leading to a cross-section ratio of $\sigma_{b\bar{b}}/\sigma_{c\bar{c}} \simeq 5\cdot 10^{-3}$ and a crossing of the c- and b-decay electron spectra at $p_t \simeq 5$ GeV.

In Figs. 5 and 6 we show the nuclear modification factor, R_{AA}, defined by $R_{AA} = P_Q(t_{\rm fin},p_t)/P_Q(0,p_t)$ (where $t_{\rm fin}$ denotes the time at the end of the mixed QGP-hadronic phase) in central and the elliptic flow,

$$v_2 = \left\langle (p_x^2 - p_y^2)/p_t^2 \right\rangle , \qquad (22)$$

in semicentral 200 AGeV Au-Au collisions. We compare the results from the T-matrix model with the parameterizations by [Wo] and [SZ] of the lQCD potentials with the those using pQCD or the resonance-model interactions of Ref. [13]. While for charm quarks for the [Wo] potential the result for R_{AA} is comparable to the upper end of the uncertainty band of the resonance-model calculation, the v_2 is slightly enhanced at low p_t. The reason for this behavior is the decrease of the transport coefficients with increasing T: While the suppression of the p_t spectra at high p_t is due to the evolution along the whole history of the fireball, leading to comparable effects at the end of the mixed phase, the anisotropic flow is mostly developed at the later stages and thus can be transferred to the heavy quarks at the end of the evolution efficiently, when the drag coefficient become larger due to the dynamical formation of the resonance states. The T-matrix result with the somewhat less attractive [SZ] potential leads to the usual ordering of the coefficients (increasing with increasing temperature) and thus shows weaker effects for both the R_{AA} and v_2 than the result of the resonance model. For b quarks the T-matrix calculations yield larger medium modifications of the p_t spectra than the resonance

model which is due to the mass effect, leading to stronger binding effects for the resonances in the T-matrix calculation. As to be expected, the effects of pQCD-based transport coefficients on the HQ spectra for both charm and bottom quarks is much weaker than the non-perturbative ones via the resonance-scattering mechanism.

4 Single-electron observables at RHIC

The last step toward a comparison of the above described model for HQ diffusion in the QGP with the single-electron p_t data from RHIC is the hadronization of the HQ spectra to D- and B-mesons and their subsequent semileptonic decay to $e^{\pm}$. Here we use the quark-coalescence model described in [38,39]. In the recent years, the coalescence of quarks in the hot and dense medium created in heavy-ion collisions has been shown to provide a successful hadronization mechanism to explain phenomena such as the scaling of hadronic elliptic-flow parameters, v_2 with the number of constituent quarks, $v_{2,h}(p_t) = n_h v_{2,q}(p_t/n_h)$, where $n_h = 2(3)$ for mesons (hadrons) denotes the number of constituent quarks contained in the hadron, h, and the large p/π ratio in Au-Au compared to p-p collisions [38, 40,41]. Quark coalescence is most efficient in the low-p_t regime where most c and b quarks combine into D and B mesons, respectively. To conserve the total HQ number, we assume that the remaining heavy quarks hadronize via (δ-function) fragmentation.

As shown in Fig. 7 the Langevin simulation of the HQ diffusion based on transport coefficients from the lQCD static potentials, followed by the combined quark-coalescence fragmentation description of hadronization to D and B mesons and their subsequent semileptonic decay, successfully accounts simultaneously for both the nuclear modification factor, R_{AA}, and the elliptic flow, v_2, of single electrons in 200 AGeV Au-Au collisions [8,7] at RHIC. The uncertainty due to the two different parameterizations of the potentials by [Wo] and [SZ] is not so large. However, the deviations from other parameterizations are bigger and will be demonstrated elsewhere [42]. The effects from the "momentum kick" of the light quarks in quark coalescence, an enhancement of both, R_{AA} and v_2, is important for the quite good agreement of both observables with the data. As can be seen from the lower panel in Fig. 7, within our model the effects from the mixing of the B-meson decay contribution to the $e^{\pm}$ spectra becomes visible in the region of $p_t \simeq 2.5$-3 GeV. A closer inspection of the time evolution of the p_t spectra shows that the suppression of high-p_t heavy quarks occurs mostly in the beginning of the time evolution, while the v_2 is built up later at temperatures close to T_c which is to be expected since the v_2 of the bulk medium is fully developed at later stages only. This effect is also pronounced for the [Wo] parameterization of the HQ potential since in this case due to resonance formation the transport coefficients become largest close to T_c.

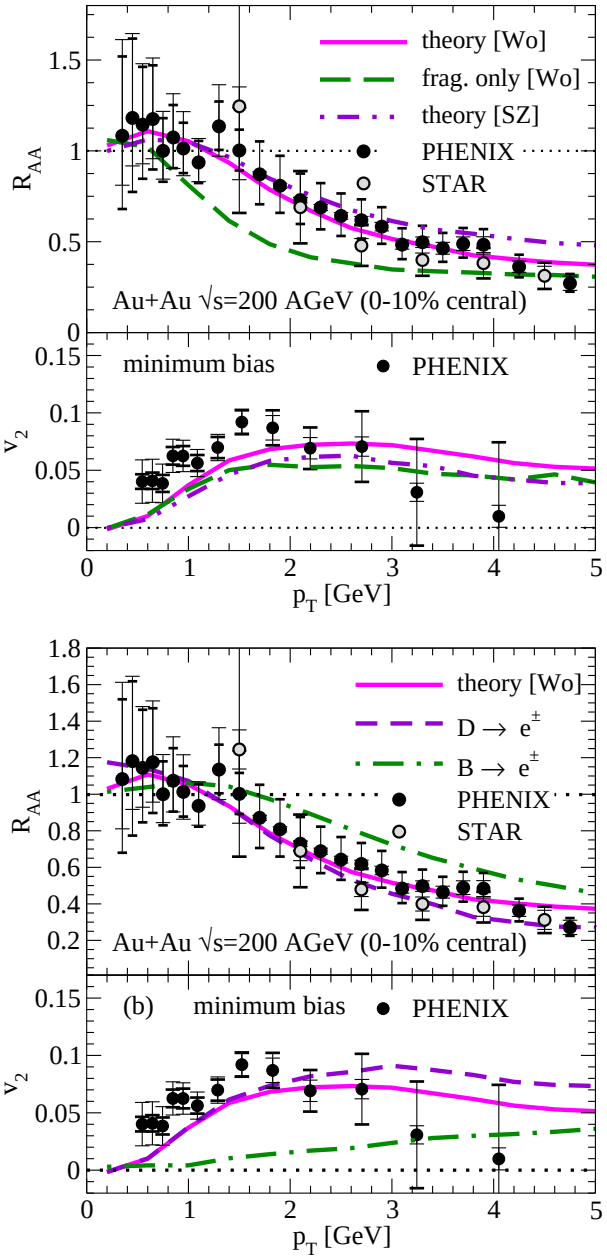

Fig. 7. (Color online) Upper panel: single-electron spectra from the T-matrix calculation of HQ diffusion in the QGP based on the [Wo] (solid line) and the [SZ] (dash-double-dotted line) parameterizations of the lQCD static HQ potential in comparison to data from the PHENIX [7] and STAR [7] collaborations in 200 AGeV Au-Au collisions at RHIC. The dashed line shows the result when only δ-function fragmentation is considered for hadronization. Lower panel: R_{AA} and v_2, as in the upper panel for the [Wo] parameterization for the electrons from D (dashed line) and B mesons (dash-dotted line) separately.

5 Conclusions and outlook

We have used static potentials from finite-temperature lQCD calculations within a Brueckner-type many-body calculation, complemented by pQCD HQ-gluon elastic-scattering matrix elements, to assess drag and diffusion coefficients for c and b quarks in the QGP in a principally parameter free approach, however plagued with large uncertainties in the determination of the relevant potential from lattice data. The diffusion of heavy quarks in the QGP is calculated with a Langevin simulation. The medium is parameterized as an expanding thermal fireball (including anisotropic flow for semicentral heavy-ion collisions) with an equation of state of a massless gas of gluons and $N_f = 2.5$ light-quark flavors. To confront this model with data on non-photonic single electrons in 200 AGeV Au-Au collisions at RHIC, we have used a combined coalescence-fragmentation model to hadronize the heavy quarks to D and B mesons which subsequently decay semi-leptonically. The resulting p_t spectra agree with recent data on the nuclear modification factor, R_{AA} and elliptic flow, v_2 quite well.

In a schematic estimate from the evaluated drag and diffusion coefficients leading to this results, based on kinetic theory using either pQCD for a weakly coupled plasma [43,44] or the strong-coupling limit applying AdS/CFT correspondence [45,46], we find values for the space-diffusion coefficient $2\pi T D_s$ = 4-6 and a viscosity to entropy-density ratio of η/s = 2-5/(4π) (to be compared to the conjectured AdS/CFT bound $(\eta/s)_{\rm min} = 1/(4\pi)$), indicating a strongly coupled (liquid like) quark-gluon plasma close to the phase transition [47].

In future works detailed studies of the uncertainties in the potential approach is necessary, in particular about the question whether a static-potential approach is justified and which in-medium potential (i.e., free or internal potential energy or combinations thereof) should be used to describe the interactions of heavy quarks within the sQGP. First steps in this direction have been made in [27] in an effective-field theory approach for non-relativistic in-medium QCD-bound states. Also an inclusion of inelastic processes like gluon bremsstrahlung which should become effective at higher p_t is mandatory for a complete picture of the in-medium behavior of heavy quarks [48].

Another step, which is quite natural, given that within our model the underlying microscopic effect of the strong coupling of the heavy quarks to the medium is the formation of resonance states close to T_c, is to substitute the quark-coalescence model with a transport-model based resonance-recombination model for hadronization in the QGP [49] which obeys the conservation laws for energy and momentum as well as the second law of thermodynamics. This model shares with quark-coalescence hadronization the phenomenologically successful feature of the scaling of v_2 with the hadrons' number of constituent quarks. Additionally it leads to scaling with the transverse kinetic energy well, provided the parton distribution and flow is calculated with a dynamically consistent scheme as the Langevin simulation discussed in the present paper [50].

This work has been supported by the U.S. National Science foundation under CAREER grant PHY-0449489 (HvH,RR), and by the Ministerio de Educación y Ciencia under grant AYA 2005-08013-C03-02 (MM).

References

1. F. Karsch, J. Phys. G **34**, S627 (2007)
2. I. Arsene et al. (BRAHMS Collaboration), Nucl. Phys. A **757**, 1 (2005)
3. B. B. Back et al. (PHOBOS Collaboration), Nucl. Phys. A **757**, 28 (2005)
4. J. Adams et al. (STAR Collaboration), Nucl. Phys. A **757**, 102 (2005)
5. K. Adcox et al. (PHENIX Collaboration), Nucl. Phys. A **757**, 184 (2005)
6. S. S. Adler et al. (PHENIX), Phys. Rev. Lett. **96**, 032301 (2006)
7. B. I. Abelev et al. (STAR Collaboration), Phys. Rev. Lett. **98**, 192301 (2007)
8. A. Adare et al. (PHENIX Collaboration), Phys. Rev. Lett. **98**, 172301 (2007)
9. N. Armesto, M. Cacciari, A. Dainese, C. A. Salgado, and U. A. Wiedemann, Phys. Lett. B **637**, 362 (2006)
10. S. Wicks, W. Horowitz, M. Djordjevic, and M. Gyulassy, Nucl. Phys. A **784**, 426 (2007)
11. S. Caron-Huot and G. D. Moore, Phys. Rev. Lett. **100**, 052301 (2008)
12. H. van Hees and R. Rapp, Phys. Rev. C **71**, 034907 (2005)
13. H. van Hees, V. Greco, and R. Rapp, Phys. Rev. C **73**, 034913 (2006)
14. M. Mannarelli and R. Rapp, Phys. Rev. C **72**, 064905 (2005)
15. H. van Hees, M. Mannarelli, V. Greco, and R. Rapp, Phys. Rev. Lett. **100**, 192301 (2008)
16. B. Svetitsky, Phys. Rev. D **37**, 2484 (1988)
17. G. D. Moore and D. Teaney, Phys. Rev. C **71**, 064904 (2005)
18. S. Godfrey and N. Isgur, Phys. Rev. D **D32**, 189 (1985)
19. M. Avila, Phys. Rev. D **49**, 309 (1994)
20. O. Kaczmarek, F. Karsch, P. Petreczky, and F. Zantow, Nucl. Phys. Proc. Suppl. **129**, 560 (2004)
21. O. Kaczmarek and F. Zantow (2005), `arXiv:hep-lat/0506019`
22. E. V. Shuryak and I. Zahed, Phys. Rev. D **70**, 054507 (2004)
23. C.-Y. Wong, Phys. Rev. C **72**, 034906 (2005)
24. D. Cabrera and R. Rapp, Phys. Rev. D **76**, 114506 (2007)
25. A. Nakamura and T. Saito, Phys. Lett. B **621**, 171 (2005)
26. M. Döring, K. Hubner, O. Kaczmarek, and F. Karsch, Phys. Rev. D **75**, 054504 (2007)
27. N. Brambilla, J. Ghiglieri, A. Vairo, and P. Petreczky, Phys. Rev. D **78** (2008)
28. O. Kaczmarek, S. Ejiri, F. Karsch, E. Laermann, and F. Zantow, Prog. Theor. Phys. Suppl. **153**, 287 (2004)
29. P. Petreczky and K. Petrov, Phys. Rev. D **70**, 054503 (2004)
30. R. H. Thompson, Phys. Rev. D **1**, 110 (1970)
31. M. I. Haftel and F. Tabakin, Nucl. Phys. A **158**, 1 (1970)
32. K. Abe et al., Phys. Rev. D **69**, 112002 (2004)
33. B. L. Combridge, Nucl. Phys. B **151**, 429 (1979)

34. P. F. Kolb, J. Sollfrank, and U. W. Heinz, Phys. Rev. C **62**, 054909 (2000), arXiv:hep-ph/0006129
35. J. Dunkel and P. Hänggi, Phys. Rev. E **71**, 016124 (2005), URL http://link.aps.org/abstract/PRE/v71/e016124
36. J. Adams et al. (STAR Collaboration), Phys. Rev. Lett. **94**, 062301 (2005)
37. A. Tai (STAR Collaboration), J. Phys. G **30**, S809 (2004)
38. V. Greco, C. M. Ko, and P. Levai, Phys. Rev. C **68**, 034904 (2003)
39. V. Greco, C. M. Ko, and R. Rapp, Phys. Lett. B **595**, 202 (2004)
40. R. C. Hwa and C. B. Yang, Phys. Rev. C **67**, 034902 (2003)
41. R. J. Fries, B. Müller, C. Nonaka, and S. A. Bass, Phys. Rev. C **68**, 044902 (2003)
42. H. van Hees, M. Mannarelli, V. Greco, and R. Rapp (2008), in preparation
43. W. Israel and J. N. Vandalas, Lett. Nuovo Cim. **19**, 887 (1970)
44. P. Danielewicz and M. Gyulassy, Phys. Rev. D **31**, 53 (1985)
45. C. P. Herzog, A. Karch, P. Kovtun, C. Kozcaz, and L. G. Yaffe, JHEP **0607**, 013 (2006)
46. J. Casalderrey-Solana and D. Teaney, Phys. Rev. D **74**, 085012 (2006)
47. R. Rapp and H. van Hees (2008), arXiv:0803.0901[hep-ph]
48. I. Vitev, A. Adil, and H. van Hees, J. Phys. G **34**, S769 (2007)
49. L. Ravagli and R. Rapp, Phys. Lett. B **655**, 126 (2007)
50. L. Ravagli, H. van Hees, and R. Rapp (2008), arXiv:0806.2055[hep-ph]